STABLE OPTIMAL DESIGN OF TWO-DIMENSIONAL ELASTIC STRUCTURES

Lars A. Krog
Institute of Mechanical Engineering, Aalborg University, Denmark

Andrej V. Cherkaev & Ismail Kucuk
Department of Mathematics, University of Utah, USA

February 26, 1998

Abstract

We study optimal design of planar structures made from anisotropic materials with an optimal composite microstructure assembled from two linearly elastic isotropic materials. The effective properties of the anisotropic materials are assumed to remain constant within pre-specified regions of the structure, and by optimality of a design we understand a design that leads to a minimum total complementary energy. The suggested formulation leads to constructions which are more stable under variation of the loading as well as variation of the parameters which describe the microstructure of the anisotropic material. We derive necessary conditions of optimality for the optimum designs of such structures and we analyze them. Numerically, we determine optimal structures for a number of examples, which are analyzed. The present paper is dedicated to Professor Z. Mróz.

1 Introduction

The present paper deals with layout optimization of planar structures assembled from two isotropic materials, characterized by different values of their elastic moduli. Given the amount of the two materials, a planar design domain Ω and the applied loads and possible supports for the structure, the layout optimization problem consists in finding a distribution of the two materials in Ω which defines a structure of maximum integral stiffness. Maximization of the integral stiffness is equivalent to minimization of the total complementary energy and thus, expressing the equilibrium problem for the structure in terms of the principle of minimum total complementary energy, we obtain the following formulation for the maximum stiffness material layout problem

$$\min_{\boldsymbol{C}(\boldsymbol{x})\in\boldsymbol{C}_{ad}} \quad \min_{\boldsymbol{\sigma}(\boldsymbol{x})\in\boldsymbol{S}(\boldsymbol{x})} \quad \frac{1}{2}\int_\Omega \boldsymbol{\sigma}(\boldsymbol{x}) : \boldsymbol{C}(\boldsymbol{x}) : \boldsymbol{\sigma}(\boldsymbol{x}) d\Omega \tag{1}$$

Here $\boldsymbol{C}(\boldsymbol{x})$ is a fourth-rank material compliance tensor, $\boldsymbol{C}_{ad}$ a set of admissible compliance tensors, and the inner minimization with respect to the stresses $\boldsymbol{\sigma}(\boldsymbol{x})$ is taken over the set $\boldsymbol{S}(\boldsymbol{x})$ of statically admissible stress fields,

$$\boldsymbol{S}(\boldsymbol{x}) = \{\ \boldsymbol{\sigma}(\boldsymbol{x})\,|\, div\boldsymbol{\sigma}(\boldsymbol{x}) + \boldsymbol{p}(\boldsymbol{x}) = 0\ in\ \Omega,\quad \boldsymbol{\sigma}(\boldsymbol{x})\boldsymbol{n}(\boldsymbol{x}) = \boldsymbol{f}(\boldsymbol{x})\ on\ ,_T\ \} \tag{2}$$

with $\boldsymbol{p}(\boldsymbol{x})$ and $\boldsymbol{f}(\boldsymbol{x})$ as body forces and surfaces tractions, $\boldsymbol{n}(\boldsymbol{x})$ as the normal vector to the surface, and $,_T$ as the traction part of the surface.

In layout optimization problems where the material properties are allowed to change from point to point in structure we generally have the discrete choice of either "*Material 1*" or "*Material 2* " at each point. Denoting the compliance tensors for the two base materials by $\boldsymbol{C}_1$ and $\boldsymbol{C}_2$ ($\boldsymbol{C}_1 < \boldsymbol{C}_2$), $\boldsymbol{C}_{ad}$ in Eq(1) becomes expressed by

$$\boldsymbol{C}(\boldsymbol{x}) = \chi(\boldsymbol{x})\boldsymbol{C}_1 + (1-\chi(\boldsymbol{x}))\,\boldsymbol{C}_2 \quad with \quad \chi(\boldsymbol{x}) = \begin{cases} 1\ if\ \boldsymbol{x} \in \Omega_1 \\ \\ 0\ if\ \boldsymbol{x} \in \Omega_2 \end{cases} \tag{3}$$

and the maximum stiffness material layout problem in Eq(1) is restated as

$$\begin{array}{l} \displaystyle\min_{\chi(\boldsymbol{x})} \quad \min_{\boldsymbol{\sigma}(\boldsymbol{x}) \in \boldsymbol{S}(\boldsymbol{x})} \quad \frac{1}{2}\int_\Omega \boldsymbol{\sigma}(\boldsymbol{x}) : (\chi(\boldsymbol{x})\boldsymbol{C}_1 + (1-\chi(\boldsymbol{x}))\boldsymbol{C}_2) : \boldsymbol{\sigma}(\boldsymbol{x}) d\Omega \\ \\ st: \quad \displaystyle\int_\Omega \chi(\boldsymbol{x}) d\Omega = V \end{array} \tag{4}$$

Here the constraint $\int_\Omega \chi(\boldsymbol{x}) d\Omega = V$ has been added to the formulation in order to avoid the trivial solution where the stiffer material $\boldsymbol{C}_1$ is used everywhere.

1.1 Introduction of a class of optimum microstructures

A numerical solution of an optimization problem generally requires a finite dimensional approximation of it. We face here the following difficulty. The optimum layout of two isotropic materials is known to be characterized by an infinitely often alternating sequence of domains occupied by each of the two materials. A finite parameter approximation to the optimization problem in Eq(4) will therefore in general be *ill-posed*, unless we extend the set of admissible compliance tensors $\boldsymbol{C}_{ad}$ to include materials with an optimum composite microstructure assembled from the two isotropic base materials.

Problems of structural optimization represent a special type of variational problem. There are many papers discussing the general variational approach to them, see for example Mróz [1]. For the design of structures of maximum rigidity it is known that optimal microstructures are found within the class of finite-rank matrix-layered composites see [2, 3, 4, 5, 6]. For maximum stiffness design problems in plane elasticity optimum microstructures are matrix-layered composites of the second and of the third rank. Here, second-rank microstructures should be used in situations where maximum rigidity against a single stress field is needed, see Gibiansky & Cherkaev [2], while third-rank microstructures should be used in situations where we need maximum rigidity against several independent stress fields or against an over domain varying macroscopic stress field (or both), see [3, 4].

Effective properties of matrix-layered composites are given by simple analytic functions of the structural parameters which describe their composition. The range of effective compliance tensors for the class of planar matrix-layered composites of given rank N is for example described by the expression

$$\boldsymbol{C}^{lamN} = \boldsymbol{C}_1 - (1-\varrho)\left((\boldsymbol{C}_1 - \boldsymbol{C}_2)^{-1} - \varrho E_1 \sum_{n=1}^{N} p_n (\boldsymbol{t}_n \otimes \boldsymbol{t}_n) \otimes (\boldsymbol{t}_n \otimes \boldsymbol{t}_n)\right)^{-1} \tag{5}$$

in which all $p_n \geq 0$, and $\sum_{n=1}^{N} p_n = 1$, see [7]. In above formula $\boldsymbol{C}_1$ and $\boldsymbol{C}_2$ represent the compliance tensors for our isotropic base materials, ϱ and E_1 the volume fraction of the stiffer material in the microstruture and its Young's modulus, respectively, while p_n and $\boldsymbol{t}_n$ are the relative layer thicknesses and the tangent vectors to the layers. In Eq(5), the dyadic product $\boldsymbol{G} = \boldsymbol{a} \otimes \boldsymbol{b}$ of two vectors $\boldsymbol{a} = [a_1, \ldots, a_n]$ and $\boldsymbol{b} = [b_1, \ldots, b_n]$ is defined as a second-rank tensor (matrix) with elements $G_{ij} = a_i b_j$. Similarly, the dyadic product of two second-rank tensors is defined as a fourth-rank tensor, and so on.

In particular, considering the case where $\boldsymbol{C}_2 = \infty$ the expression for the effective compliance tensor in Eq(5) describes the effective compliance of a material weakened by a system of infinitesimal holes. In this situation Eq(5) simplifies to

$$\boldsymbol{C}^{lamN} = \boldsymbol{C}_1 + \boldsymbol{\Delta}^{-1} \tag{6}$$

with

$$\boldsymbol{\Delta} = \frac{\varrho E_1}{1-\varrho} \sum_{n=1}^{N} p_n (\boldsymbol{t}_n \otimes \boldsymbol{t}_n) \otimes (\boldsymbol{t}_n \otimes \boldsymbol{t}_n) \tag{7}$$

To describe the fourth-rank tensors involved in above expressions, it is convenient to introduce the following orthogonal basis of second-rank tensors

$$\boldsymbol{a}_1 = \frac{1}{\sqrt{2}}\begin{bmatrix} 1 & 0 \\ 0 & -1 \end{bmatrix}, \quad \boldsymbol{a}_2 = \frac{1}{\sqrt{2}}\begin{bmatrix} 0 & 1 \\ 1 & 0 \end{bmatrix}, \quad \boldsymbol{a}_3 = \frac{1}{\sqrt{2}}\begin{bmatrix} 1 & 0 \\ 0 & 1 \end{bmatrix} \tag{8}$$

In this basis, any symmetric second-rank tensor is represented as a vector, and any symmetric fourth-rank tensor as a symmetric 3x3 matrix. The fourth-rank tensor $\boldsymbol{\Delta}$ in Eq(7) may for example be represented as

$$\overline{\overline{\boldsymbol{\Delta}}} = \frac{\varrho E_1}{2(1-\varrho)} \sum_{n=1}^{N} p_n \begin{bmatrix} \dfrac{1+\cos(4\theta_n)}{2} & \dfrac{\sin(4\theta_n)}{2} & -\cos(2\theta_n) \\ & \dfrac{1-\cos(4\theta_n)}{2} & -\sin(2\theta_n) \\ & & 1 \end{bmatrix} \tag{9}$$

where θ_n represent the orientation of the n-layer in the microstructure, such that the tangent vector to the layers becomes defined as $\boldsymbol{t}_n = \{-sin\theta_n, cos\theta_n\}^T$.

Finally, we note that the matrix $\overline{\overline{\boldsymbol{\Delta}}}$ in Eq(9) has two linear invariants called the spherical trace $\mathbf{Tr_s}$ and the deviatoric trace $\mathbf{Tr_d}$. These quantities are defined as

$$\mathbf{Tr_s}(\overline{\overline{\boldsymbol{\Delta}}}) = [\Delta_{33}] = \frac{\varrho E_1}{2(1-\varrho)} \tag{10}$$

and

$$\mathbf{Tr_d}(\overline{\overline{\boldsymbol{\Delta}}}) = [\Delta_{11}] + [\Delta_{22}] = \frac{\varrho E_1}{2(1-\varrho)} \tag{11}$$

Below, we use the notation

$$c = \frac{\varrho E_1}{2(1-\varrho)}. \tag{12}$$

Furthermore, the inverse statement is also true. Hence, any matrix $\overline{\overline{\boldsymbol{\Delta}}}$ that

(1) is strongly positive definite: $\det \overline{\overline{\boldsymbol{\Delta}}} > 0$

(2) has two linear invariants as in Eqs(10, 11),

admits the representation given in Eq(9), (see Avellaneda & Milton[4]).

1.2 A well-posed optimal design problem

Application of Eq(5) allow us to obtain a *well-posed* finite parameter approximation to the maximum stiffness material layout problem in Eq(4). In this approximation we consider a division of the design domain Ω into a finite number of sub-domains Ω_i, $i = 1, \dots, I$, and we then allow an optimal matrix-layered composite to be formed within each of these sub-domains. Hence, we arrive at the formulation

$$\begin{aligned} &\min_{\boldsymbol{C}_i \in \boldsymbol{C}^{lam3}} \quad \min_{\boldsymbol{\sigma}(\boldsymbol{x}) \in \boldsymbol{S}(\boldsymbol{x})} \quad \sum_{i=1}^{I} \frac{1}{2} \int_{\Omega_i} \boldsymbol{\sigma}(\boldsymbol{x}) : \boldsymbol{C}_i : \boldsymbol{\sigma}(\boldsymbol{x}) d\Omega \\ &st: \quad \sum_{i=1}^{I} \varrho^i v^i = V \end{aligned} \tag{13}$$

If all density variables ϱ_i in the above formulation are allowed to vary continuously between 0 and 1, then the design model covers designs of the type where we in each sub-domain Ω_i allow the use of pure "material 1", pure "material 2" or an optimum composite mixture of the two isotropic base materials. Please note that, since the stress field in the general case will vary over the sub-domains Ω_i, optimum microstructures for the above problem are found within the class matrix-layered composites of the third rank denoted by $\boldsymbol{C}^{lam3}$, see Avellaneda[3].

Homogenization approach to topology optimization: Taking the size of the sub-domains Ω_i in Eq(13) to correspond to the grid size in a finite element mesh and taking the material in each of these sub-domains as an orthogonal second-rank matrix-layered composite in which one of the base materials is chosen as a very compliant material (representing void), above formulation has been successfully applied to the solution of topology optimization problems for continuum structures, see e.g. Bendsøe [8], [9]. In this setting the optimum material layout problem in Eq(13) is known as the homogenization approach to topology optimization. For an overview over the field of layout and topology optimization for continuum structures the reader is refer to Bendsøe [9] and Rozvany, Bendsøe & Kirsch [10].

1.3 Stable optimization design problem

The maximum stiffness material layout optimization problem described above, and especially the use of orthogonal second-rank matrix-layered composites in the homogenization approach to topology optimization is associated with a number of problems

- One of these problems is the use of composite materials which are allowed to change composition with an arbitrary fine scale. The nearly point-wise variation of material properties makes the final design extremely difficult to manufacture.
- Another problem is related to the use of second-rank matrix-layered composites which, being anisotropic, "concentrate" their capacity of resistance along the direction of the expected stress field; because of this they do not resist at all to a stress field directed orthogonal to the expected one. The optimal construction is therefore extremely sensitive to changes in both the loading and in the orientation of the microstructures, and small perturbations of these parameters may lead to an essential reduction of its rigidity.
- A third problem is that the macroscopic stress field actually will vary over the domain of even an element in a finite element formulation. Optimum microstructures are therefore not found within the class of orthogonal second-rank matrix-layered composites.

All of these problems are eliminated by considering the formulation in Eq(13). The key to obtain a *well-posed* stable formulation of the planar maximum stiffness material layout problem is the use of third-rank matrix layered composites. The effective compliance properties of these composites are described by Eq(5) taking $N = 3$. We note that if none of the parameters p_1, p_2, p_3 are zero, then the compliance tensor for the third-rank composite is finite, even if the compliance of the enveloped material $\boldsymbol{C}_2$ is infinite. The third-rank microstructure, and thereby the structure made from such a material, is therefore much more stable upon changes in the loading and in the layer orientation. Second-rank laminates as well as simple laminates correspond to degeneration of the high-rank composites. Roughly speaking, the layers of strong material in the third-rank microstructure form triangles instead of rectangles, and that provides the uniform rigidity to this class of microstructures.

Further stability may be added to the structure by considering optimum design against several independent loading situations. A natural generalization of Eq(13) would therefore be to consider the following simple multiple load case formulation

$$
\begin{aligned}
&\min_{\boldsymbol{C}_i \in \boldsymbol{C}^{lam3}} \quad \min_{\boldsymbol{\sigma}_j(\boldsymbol{x}) \in \boldsymbol{S}_j(\boldsymbol{x})} \quad \sum_{j=1}^{J}\sum_{i=1}^{I} \frac{1}{2}\int_{\Omega_i} \boldsymbol{\sigma}_j(\boldsymbol{x}) : \boldsymbol{C}_i : \boldsymbol{\sigma}_j(\boldsymbol{x}) d\Omega \\
&st: \quad \sum_{i=1}^{I} \varrho^i v^i = V
\end{aligned}
\tag{14}
$$

Here the outer minimization over $\boldsymbol{C}_i$, $i = 1, \ldots, I$, represent the optimum design problem, while the inner minimization over $\boldsymbol{\sigma}_j$, $j = 1, \ldots, J$, represent the equilibrium problems for J independent loading situations. Again optimum microstructures are found within the class of third-rank matrix-layered composites.

2 The Formulation

We consider here a new formulation of the optimization problem in Eq(14) that is especially suited for dealing with energy optimization problems involving multiple loads or/and domain-wise constant material properties.

The formulation introduces a measure U_i for the sum of energies in a sub-domain Ω_i. To define this measure we start by rewriting the energy density $u_j(\boldsymbol{x})$ for load case number j as

$$
u_j(\boldsymbol{x}) = \frac{1}{2}\boldsymbol{\sigma}_j(\boldsymbol{x}) : \boldsymbol{C}(\boldsymbol{x}) : \boldsymbol{\sigma}_j(\boldsymbol{x}) = \mathbf{Tr}(\overline{\overline{\boldsymbol{C}}}(\boldsymbol{x})\ \overline{\overline{\boldsymbol{z}}}_j(\boldsymbol{x})) \tag{15}
$$

Here $\overline{\overline{\boldsymbol{z}}}_j(\boldsymbol{x})$ is a symmetric, positive definite 3x3 matrix corresponding to the fourth-rank tensor $(\boldsymbol{\sigma}_j(\boldsymbol{x}) \otimes \boldsymbol{\sigma}_j(\boldsymbol{x}))/2$, represented in the tensor basis given in Eq(8). Next, introducing symmetric, positive definite 3x3 matrices $\overline{\overline{\boldsymbol{Z}}}_i$, defined as

$$
\overline{\overline{\boldsymbol{Z}}}_i = \sum_{j=1}^{J} \int_{\Omega_i} \overline{\overline{\boldsymbol{z}}}_j(\boldsymbol{x}) d\Omega \quad , \quad i = 1, \ldots, I \tag{16}
$$

whereby the sum of energies U_i in a sub-domain Ω_i, characterized by its constant material compliance matrix $\overline{\overline{\boldsymbol{C}}}_i$, is determined as

$$
U_i = \mathbf{Tr}(\overline{\overline{\boldsymbol{C}}}_i \overline{\overline{\boldsymbol{Z}}}_i) \tag{17}
$$

Note, that the matrices $\overline{\overline{\boldsymbol{Z}}}_i$ introduced in Eq(16) collect all information about the fields $\overline{\overline{\boldsymbol{z}}}_j(\boldsymbol{x})$, $j = 1, \ldots, J$, (and thereby the stress fields) in a sub-domain Ω_i. Furthermore, they allow for a simple definition of the multiple load domain energy measure U_i in Eq(17), and they give us a simple unified formulation for adressing problems with multiple loads and domain-wise constant material properties.

In addition to the matrices $\overline{\overline{\boldsymbol{Z}}}_i$, it is convenient to introduce the square root of these matrices as positive definite 3x3 matrices which fulfill the relation $\overline{\overline{\boldsymbol{S}}}_i^2 = \overline{\overline{\boldsymbol{Z}}}_i$. To this end we note that any symmetric, positive definite matrix admits a representation via its non-negative eigenvalues ζ^k and its corresponding eigenvectors $\overline{\boldsymbol{\alpha}}^k$

which fulfill the orthonormality condition $\overline{\boldsymbol{\alpha}}_i^T\overline{\boldsymbol{\alpha}}_j = \delta_{ij}$. The 3x3 matrix $\overline{\overline{\boldsymbol{Z}}}$ may for example be represented as

$$\overline{\overline{\boldsymbol{Z}}} = \sum_{k=1}^{3} \zeta_k \overline{\boldsymbol{\alpha}}_k \overline{\boldsymbol{\alpha}}_k^T \quad , \quad \zeta_k > 0, \tag{18}$$

and the square root of this matrix hereby is equal to

$$\overline{\overline{\boldsymbol{S}}} = \sum_{k=1}^{3} \lambda_k \overline{\boldsymbol{\alpha}}_k \overline{\boldsymbol{\alpha}}_k^T \quad , \quad \lambda_k = \sqrt{\zeta^k} \tag{19}$$

such that

$$\overline{\overline{\boldsymbol{Z}}} = \overline{\overline{\boldsymbol{S}}}^2 = \sum_{i=1}^{3}\sum_{j=1}^{3} \lambda_i\lambda_j \overline{\boldsymbol{\alpha}}_i \underbrace{\overline{\boldsymbol{\alpha}}_i^T \overline{\boldsymbol{\alpha}}_j}_{\delta_{ij}} \overline{\boldsymbol{\alpha}}_j^T = \sum_{i=1}^{3} \lambda_i^2 \overline{\boldsymbol{\alpha}}_i \overline{\boldsymbol{\alpha}}_i^T \tag{20}$$

Using the above definitions the multiple load domain energy measure in Eq(17) can be expressed as

$$U = \mathbf{Tr}(\overline{\overline{\boldsymbol{C}}}\ \overline{\overline{\boldsymbol{S}}}^2) = \sum_{k=1}^{3} (\lambda_k \overline{\boldsymbol{\alpha}}_k^T)\overline{\overline{\boldsymbol{C}}}(\lambda_k \overline{\boldsymbol{\alpha}}_k) \tag{21}$$

and the optimization problem in Eq(14) may now be stated in the following form

$$\min_{\boldsymbol{\sigma}_j(\boldsymbol{x}) \in \boldsymbol{S}_j(\boldsymbol{x})} \ \min_{\varrho_i} \ \min_{\overline{\overline{\boldsymbol{\Delta}}}_i} \ \mathbf{Tr}\left(\sum_{i=1}^{I} \overline{\overline{\boldsymbol{C}}}_i \overline{\overline{\boldsymbol{S}}}_i^2\right) \quad , \quad i = 1, \ldots, I \tag{22}$$

subject to

$$\sum_{i=1}^{I} \varrho_i v_i = V \tag{23}$$

and

$$\mathbf{Tr_s}\overline{\overline{\boldsymbol{\Delta}}}_i = \mathbf{Tr_d}\overline{\overline{\boldsymbol{\Delta}}}_i = c \quad , \quad i = 1, \ldots, I \tag{24}$$

The minimization with respect to the configuration of the microstructure is here treated as a minimization problem for arbitrary 3x3 matrices $\overline{\overline{\boldsymbol{\Delta}}}_i$ subject to linear constraints on their spherical and deviatoric trace. These constraints assure that the obtained matrices $\overline{\overline{\boldsymbol{\Delta}}}_i$ admits a representation (9). Furthermore, we see that the minimization with respect to both the material densities ϱ_i and the configuration of the microstructure has been moved to the other side of the equilibrium problem. The problem of finding the optimum configuration of the microstructures has hereby been transformed into a series of local optimization problems (one for each of the sub-domains Ω_i). Each of these local problems consists in finding the matrix $\overline{\overline{\boldsymbol{\Delta}}}_i$ which minimizes the domain energy measure U_i for the sub-domain subject to the two linear constraints on the spherical and deviatoric trace of $\overline{\overline{\boldsymbol{\Delta}}}_i$. Considering Eq(21) we see that the optimum microstructure indeed is one which minimimizes a sum of complementary energies associated with three orthogonal stress fields $\boldsymbol{s}_k = \lambda_k \boldsymbol{\alpha}_k$, $k = 1, \ldots, 3$.

2.1 Solution of local problems

In order to find the optimal configuration of the microstructures throughout a design domain Ω we could express the parameters which describe the microstructure in each of the sub-domains Ω_i via the acting stresses in the domain using the necessary conditions of optimality. In Eq(22) this problem was transformed into a series of local problems, each consisting in finding a matrix $\overline{\overline{\boldsymbol{\Delta}}}_i$ which minimizes a functional of the form (17) subject to two linear constraints as given in Eqs(10)-(11). This problem is in the following solved via necessary conditions of optimality.

We start by forming an extended Lagrangian function by adding the two linear constraints in Eqs(10)-(11) to our objective function in Eq(17) with Lagrange multipliers μ_1 and μ_2,

$$I = \ \mathbf{Tr}\left(\left(\overline{\overline{\boldsymbol{C}}}_1 + \overline{\overline{\boldsymbol{\Delta}}}_i^{-1}\right)\overline{\overline{\boldsymbol{S}}}_i^2\right) + \mu_1(\ \mathbf{Tr_s}(\overline{\overline{\boldsymbol{\Delta}}}_i) - c) + \mu_2(\ \mathbf{Tr_d}(\overline{\overline{\boldsymbol{\Delta}}}_i) - c) \tag{25}$$

Suppose first that the material density is fixed. The necessary optimality conditions consist of a set of stationarity conditions for the extended Lagrangian function with respect to the components $[\Delta_{ij}]$ of the 3x3 matrix $\overline{\overline{\boldsymbol{\Delta}}}_i$.

Define the derivative of a scalar function $\phi(\overline{\overline{\boldsymbol{A}}})$ with respect to a matrix $\overline{\overline{\boldsymbol{A}}}$ with components $[a_{ij}]$ as as a matrix $\overline{\overline{\boldsymbol{B}}}$ with components $[b_{ij}] = \partial\phi(\overline{\overline{\boldsymbol{A}}})/\partial[a_{ji}]$, we observe

$$\frac{\partial}{\partial\overline{\overline{\boldsymbol{\Delta}}}_i}\ \mathbf{Tr}(\overline{\overline{\boldsymbol{\Delta}}}_i^{-1}\overline{\overline{\boldsymbol{S}}}_i^2) = -\left(\overline{\overline{\boldsymbol{\Delta}}}_i^{-1}\overline{\overline{\boldsymbol{S}}}_i\right)\left(\overline{\overline{\boldsymbol{\Delta}}}_i^{-1}\overline{\overline{\boldsymbol{S}}}_i\right)^T \tag{26}$$

$$\frac{\partial}{\partial\overline{\overline{\boldsymbol{\Delta}}}_i}\ \mathbf{Tr_s}(\overline{\overline{\boldsymbol{\Delta}}}_i) = diag\,[\ 0,\ 0,\ 1\ ] \tag{27}$$

$$\frac{\partial}{\partial\overline{\overline{\boldsymbol{\Delta}}}_i}\ \mathbf{Tr_d}(\overline{\overline{\boldsymbol{\Delta}}}_i) = diag\,[\ 1,\ 1,\ 0\ ] \tag{28}$$

We note that Eq(26) holds at least in the situation where the matrices $\overline{\overline{\boldsymbol{\Delta}}}_i$ and $\overline{\overline{\boldsymbol{S}}}_i$ are both symmetric.

Using above results the stationarity conditions for the extended Lagrangian function I with respect to the components $[\Delta_{ij}]$ of the matrix $\overline{\overline{\boldsymbol{\Delta}}}_i$ is summarized by the matrix equation

$$\frac{\partial I}{\partial\overline{\overline{\boldsymbol{\Delta}}}_i} = -\left(\overline{\overline{\boldsymbol{\Delta}}}_i^{-1}\overline{\overline{\boldsymbol{S}}}_i\right)\left(\overline{\overline{\boldsymbol{\Delta}}}_i^{-1}\overline{\overline{\boldsymbol{S}}}_i\right)^{\mathbf{T}} + \overline{\overline{\boldsymbol{A}}}_i\ \overline{\overline{\boldsymbol{A}}}_i^{\mathbf{T}} = 0 \tag{29}$$

where

$$\overline{\overline{\boldsymbol{A}}}_i = diag\,[\ \sqrt{\mu_2},\ \sqrt{\mu_2},\ \sqrt{\mu_1}\ ]_i \tag{30}$$

Here, the positiveness and the symmetry of the involved matrices ensure the uniqueness of the square root of the matrix $\overline{\overline{\boldsymbol{A}}}_i$ and therefore also the uniqueness of the the following equation for the optimal $\overline{\overline{\boldsymbol{\Delta}}}_i$ matrix

$$\overline{\overline{\boldsymbol{\Delta}^*}}_i = \overline{\overline{\boldsymbol{S}}}_i\ \overline{\overline{\boldsymbol{A}}}_i^{-1} \tag{31}$$

In order to determine the Lagrange multipliers μ_1 and μ_2 which defines the matrix $\overline{\overline{\boldsymbol{A}}}_i$ in Eq(31), we take the spherical and deviatoric trace of the above expression for the optimal $\overline{\overline{\boldsymbol{\Delta}}}_i$ matrix, and use the constrains which these traces must fulfill, see Eqs(10)-(11). Taking the spherical trace of the above expression for optimal $\overline{\overline{\boldsymbol{\Delta}}}_i$ and setting this trace equal to the constant c_i defined in Eq(12), we obtain

$$\mathbf{Tr_s}(\overline{\overline{\boldsymbol{\Delta}^*}}_i) = \mathbf{Tr_s}\left(\overline{\overline{\boldsymbol{S}}}_i\ \overline{\overline{\boldsymbol{A}}}_i^{-1}\right) = \frac{\mathbf{Tr_s}(\overline{\overline{\boldsymbol{S}}}_i)}{\sqrt{\mu_1}} = c_i \tag{32}$$

whereby

$$\sqrt{\mu_1} = \frac{1}{c_i}\ \mathbf{Tr_s}(\overline{\overline{\boldsymbol{S}}}_i) \tag{33}$$

and similarly we find

$$\sqrt{\mu_2} = \frac{1}{c_i}\ \mathbf{Tr_d}(\overline{\overline{\boldsymbol{S}}}_i) \tag{34}$$

Finally, substituting the Lagrange multipliers given in Eqs(33)-(34) and the inverse of the expression for $\overline{\overline{\boldsymbol{\Delta}^*}}_i$ in Eq(31) back into Eq(25) we find the minimal multiple load domain energy measure (for fixed volume fraction) as

$$U_i^* = \frac{2(1-\varrho_i)}{\varrho_i E_1}\left[\ \mathbf{Tr_s}^2(\overline{\overline{\boldsymbol{S}}})_i +\ \mathbf{Tr_d}^2(\overline{\overline{\boldsymbol{S}}}_i)\right] +\ \mathbf{Tr}\ (\overline{\overline{\boldsymbol{C}}}_1\overline{\overline{\boldsymbol{S}}}_i^2) \tag{35}$$

2.2 Optimal volume fractions

Also the problem of finding the optimal material densities ϱ_i may be solved analytically via necessary conditions of optimality. To this end we form an extended lagrangian function, obtained by summing the minimum multiple load domain energy measures U_i^* (found by solving the local problems) and then add the volume constraint in Eq(23) with a Lagrange multiplier γ, i.e.,

$$I = \sum_{i=1}^{I} U_i^* + \gamma\left(\sum_{i=1}^{I}\varrho_i v_i - V\right) \tag{36}$$

Introducing minimum multiple load domain energy measures U_i^* from Eq(35) into the above expression, we get

$$I = \sum_{i=1}^{I}\left(\frac{2(1-\varrho_i)}{\varrho_i E_1}\left(\mathbf{Tr_s}^2(\overline{\overline{\boldsymbol{S}}}_i) + \mathbf{Tr_d}^2(\overline{\overline{\boldsymbol{S}}}_i)\right) + \mathbf{Tr}(\overline{\overline{\boldsymbol{C}}}_1\ \overline{\overline{\boldsymbol{S}}}_i^2)\right) + \gamma\left(\sum_{i=1}^{I}\varrho_i v_i - V\right) \tag{37}$$

which by differentiating with respect to a material density ϱ_i gives us the necessary optimality condition

$$\frac{\partial I}{\partial \varrho_i} = -\left(\frac{2}{\varrho_i E_1} + \frac{2(1-\varrho_i)E_1}{(\varrho_i E_1)^2}\right)\left(\mathbf{Tr_s}^2(\overline{\overline{\boldsymbol{S}}}_i) + \mathbf{Tr_d}^2(\overline{\overline{\boldsymbol{S}}}_i)\right) + \gamma v_i = 0 \tag{38}$$

This condition is easily solve for the optimal material densities,

$$\varrho_i^* = \sqrt{\frac{2\left(\mathbf{Tr_s}^2(\overline{\overline{\boldsymbol{S}}}_i) + \mathbf{Tr_d}^2(\overline{\overline{\boldsymbol{S}}}_i)\right)}{\gamma E_1 v_i}}\quad ,\quad i = 1, \ldots, I \tag{39}$$

where the Lagrange multiplier γ should be choosen such that the volume constraint in Eq(23) is fulfilled.

Finally substituting the expression for the optimum material density ϱ_i^* into Eq(35) we obtain the minimum multiple load domain energy measure for optimal material densities

$$U_i^{**}(\overline{\overline{\boldsymbol{S}}}_i) = \begin{cases} \dfrac{2B}{E_1}\left(\sqrt{\dfrac{\gamma E_1 v_i}{2B}} - 1\right) + \mathbf{Tr}(\overline{\overline{\boldsymbol{C}}}_1\ \overline{\overline{\boldsymbol{S}}}_i^2)\ , & if \quad \varrho_i^* < 1 \\ \mathbf{Tr}(\overline{\overline{\boldsymbol{C}}}_1\ \overline{\overline{\boldsymbol{S}}}_i^2)\ , & if \quad \varrho_i^* = 1 \end{cases} \tag{40}$$

whith

$$B = \left(\mathbf{Tr_s}^2(\overline{\overline{\boldsymbol{S}}}_i) + \mathbf{Tr_d}^2(\overline{\overline{\boldsymbol{S}}}_i)\right) \tag{41}$$

The equation for $U_i^{**}(\overline{\overline{\boldsymbol{S}}}_i)$ describes the quasi-convex envelope of the energy see for example [7, 11], that is the minimal energy stored in any body under given load. The specific energy stored in the material is equal to $U_i^{**}(\overline{\overline{\boldsymbol{S}}}_i)/\varrho_i(\overline{\overline{\boldsymbol{S}}}_i)$.

3 Numerics

In this section we consider examples of optimal design of planar structures with domain-wise constant material properties. Taking as design variables the parameters which characterize a third-rank matrix-layered composite within each of a number of prespecified sub-domains of the structure, we determine the structures with minimum total complementary energy. For the present studies it was chosen to solve the optimization problems by means of design sensitivity analysis and a method of mathematical programming, rather that to apply the necessary conditions optimality develloped in the previous section.

At this point we note that a parameterization of the effective compliance tensor in terms of layer densities p_n and layer orientations θ_n, see Eqs(42), are known to lead to local minima of the total complementary energy, see e.g. Pedersen [12]. For the solution of the present problem we therefore choose a parameterization of the effective compliance tensor in terms of so-called moment variables, see e.g. Francfort & Murat [11] and Avellaneda & Milton [4]. This parameterization of the effective compliance tensor is, due to the convexity of the complementary energy in terms of the moments, perfectly suited for an iterative hierarchical design approach where the global distribution of material (the ϱ parameters) is improved in an outer loop while the optimal configuration of the microstructures are found numerically as solutions to a set of inner optimization problems in the moment variables. For a discussion of the convexity properties of the moment formulation the reader is referred to Lipton [5], while examples on application of moment formulations to solution of topology optimization problems can be found in Lipton & Soto [6]; Lipton & Diaz [13]; Krog & Olhoff [14].

For the sake of completeness we shall in the following give first a brief description of the moment formulation, before we consider examples of optimal material design for structures with domain-wise constant material properties.

3.1 The moment formulation

A parameterization of the effective compliance matrix in terms of moments is obtained by simply applying the following variable substitutions to Eqs(9)

$$
\begin{aligned}
m_1 &= \sum_{n=1}^{N} p_n cos(2\theta_n) \quad ; \quad m_2 = \sum_{n=1}^{N} p_n sin(2\theta_n) \\
m_3 &= \sum_{n=1}^{N} p_n cos(4\theta_n) \quad ; \quad m_4 = \sum_{n=1}^{N} p_n sin(4\theta_n)
\end{aligned}
\tag{42}
$$

whereby the 3x3 matrix representation of the effective compliance tensor in Eq(5) may be written as

$$
\overline{\overline{\boldsymbol{C}}}^{lamN} = \overline{\overline{\boldsymbol{C}}}_1 - (1-\varrho)\left(\left(\overline{\overline{\boldsymbol{C}}}_1 - \overline{\overline{\boldsymbol{C}}}_2\right)^{-1} - \varrho E_1 \overline{\overline{\boldsymbol{M}}}\right)^{-1} \tag{43}
$$

with

$$
\overline{\overline{\boldsymbol{M}}} = \frac{1}{2}\begin{bmatrix} \frac{1+m_3}{2} & \frac{m_4}{2} & -m_1 \\ & \frac{1-m_3}{2} & -m_2 \\ & & 1 \end{bmatrix} \tag{44}
$$

The moment variables $\boldsymbol{m} = \{m_1, \ldots, m_4\}$ introduced above are not physical variables and they must therefore fulfill certain restrictions. This set of restrictions is easily established considering the case where we range over all possible layer directions. In this case the moments become

$$
\begin{aligned}
m_1 &= \int_0^{2\pi} p(\theta) cos(2\theta) d\theta \quad ; \quad m_2 = \int_0^{2\pi} p(\theta) sin(2\theta) d\theta \\
m_3 &= \int_0^{2\pi} p(\theta) cos(4\theta) d\theta \quad ; \quad m_4 = \int_0^{2\pi} p(\theta) sin(4\theta) d\theta
\end{aligned}
\tag{45}
$$

With the above definition of the moments and the solution to the trigonometric moment problem, see Krein & Nudelmann [15], we easily get the set of feasible moments

$$
H = \left\{ \boldsymbol{m} \in \Re^4 \;\middle|\; \begin{array}{c} m_1^2 + m_2^2 \leq 1 \quad , \quad -1 \leq m_3 \leq 1 \ , \\ \dfrac{2m_1^2}{1+m_3} + \dfrac{2m_2^2}{1-m_3} + \dfrac{m_4^2 - 4m_1m_2m_4}{1-m_3^2} \leq 1 \end{array} \right\} \tag{46}
$$

The expressions in Eqs(43)-(46) gives us the effective properties for the set of all finite-rank matrix-layered composites. However, in general we do not need to consider more than third-rank microstructures, since the effective compliance tensor for any planar microstructure can be realized using only tree layered directions. A method for identifying a third-rank microstructure which corresponds to a given set of moments can be found in Lipton [5].

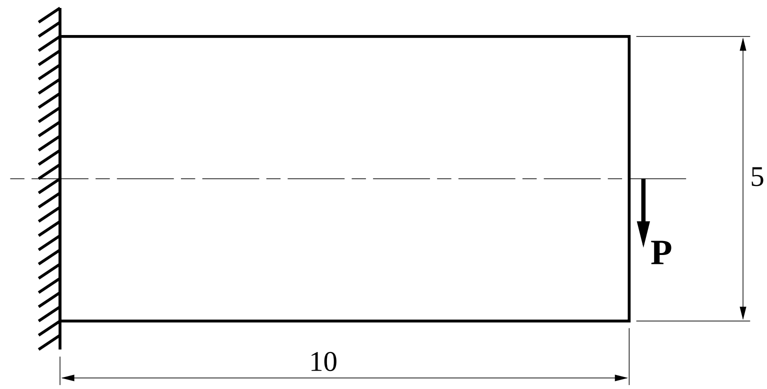

Figure 1: Design domain, load and boundary conditions.

Applying above parameterization for the effective compliance matrix our optimal material layout problem may be stated as

$$\min_{\varrho_i} \quad \min_{\boldsymbol{\sigma}_j \in \boldsymbol{S}_j} \min_{\boldsymbol{m}_i \in H} \quad \sum_{i=1}^{I} \mathbf{Tr}\left(\overline{\overline{\boldsymbol{C}}}_i \overline{\overline{\boldsymbol{Z}}}_i\right) \tag{47}$$

subject to

$$\sum_{i=1}^{I} \varrho_i v_i = V \tag{48}$$

Here the outer optimization problem determines the macro-scopic distribution material in the structure, while the inner optimization problem determines the microstructure in each of the sub-domains Ω_i. We note that the inner optimization problem actually may be solved as a set of smaller minimization problems, one for each of the sub-domains Ω_i.

3.2 Example

Applying the moment formulation described in the previous section, we now consider a series of examples of optimal design of planar structures with domain-wise constant material properties. A plane design domain which is subjected to a single concentrated load and supported as shown in Figure 1 is considered, and by applying a symmetry condition we analyze only the upper half of the structure. The upper half of the structure is initially discretized into 8x32 four-node anisotropic finite elements and then divided into a number of sub-domains which we will assume to have constant material properties. We use as design variables the parameters which characterize a third matrix-layered composite in each of the sub-domains of the structure, and study the performance of the optimal designs as the number of these sub-domains is increased.

In all examples, the available amount of the stiffer material in the matrix-layered composite is set to be 40% of the design domain volume, and we specify the stiffness ratio between the stiff and the soft material in the microstructure to be 100, while both materials are taken to have the same Poisson's ration of 0.3.

Table 1 shows the total complementary energy for a series of optimal designs, obtained using 1, 2 and 4 horizontal sub-domains with 1, 2, 4, 8 and 16 vertical sub-domains, respectively. As expected, it is seen that the total complementary energy decreases when the number of sub-domains with independent material properties are increased.

	1	2	4	8	16
1	1.000	0.881	0.827	0.794	0.774
2	0.765	0.658	0.598	0.565	0.548
4	0.679	0.588	0.537	0.508	0.493

Table 1: Normalized total complementary energy for optimal designs.

Remark: In particular, we observe the importance of actual division of the structure into sub-domains. Optimally this division of the structure should therefore be obtained as part of the solution to a more general optimization problem, rather than be performed manually.

The pictures of the optimal designs are shown in Figure 2-6. It should be stressed that the pictures are only illustrations of the optimum microstructures. The distance between the layers has been used to illustrate the different length scales in the third-rank microstructure, while layer thicknesses are used to illustrate the density of material in each level of the third-rank microstructure. In reality both the distance between layers and the layer thicknesses should be infinitely small. Also it should be mentioned that the microstructures shown represent just one of the possible realizations of a third-rank microstructure that will give exactly the same set of effective material properties. Indeed, the formula 4 does not specify which layer is "thicker", and therefore there are at least three equal solutions of it.

From the series of pictures of the optimal designs it becomes clear that the stiff material will be concentrated in the areas where the stress field has singularities. That is where the concentrated load is applied and where the beam is attached to the rigid support. The smaller the sub-domains of the structure becomes, the higher becomes the concentration of the stiff material in these areas.

Next, studying the microstructure of the material we see that the optimal material everywhere has a third-rank microstructure. Also we see that the stronger layers of the stiff material practically speaking becomes co-aligned with what we should expect to be the principal stress directions in a domain. That is at ∓ 45degrees near the core of the beam where we have large shearing stresses and at zero degrees 0 in areas where we have large bending stresses. Another effect which might be observed is how the layers of the stiff material rotate when we get closer to the tip of the beam in order to catch the concentrated load at this point.

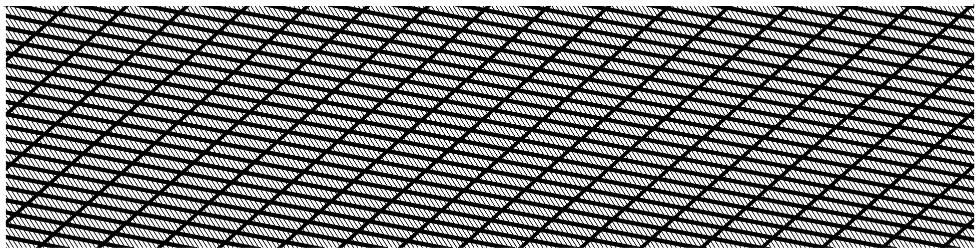

(a)

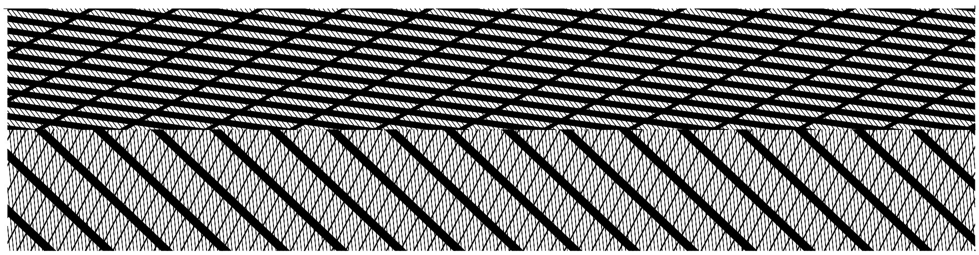

(b)

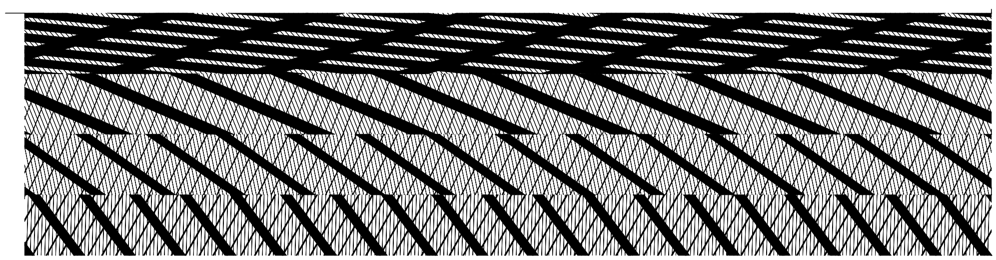

(c)

Figure 2: Optimal designs obtained using 1x1, 2x1, and 4x1 domains with constant material properties.

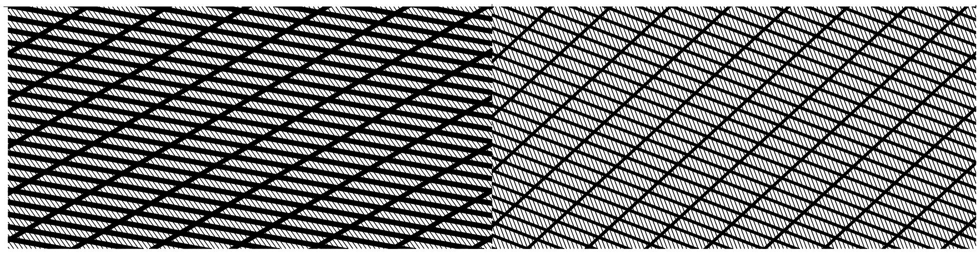

(a)

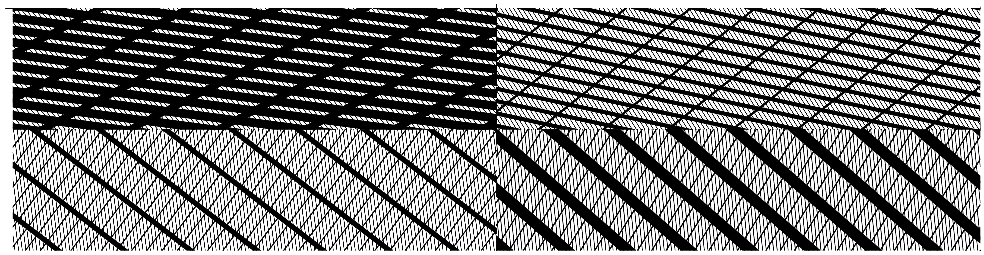

(b)

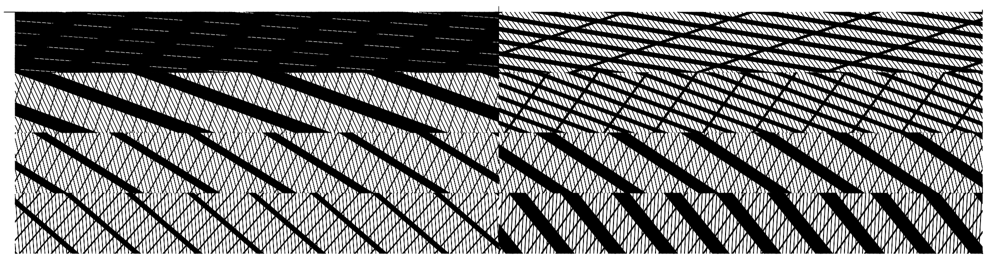

(c)

Figure 3: Optimal designs obtained using 1x2, 2x2, and 4x2 domains with constant material properties.

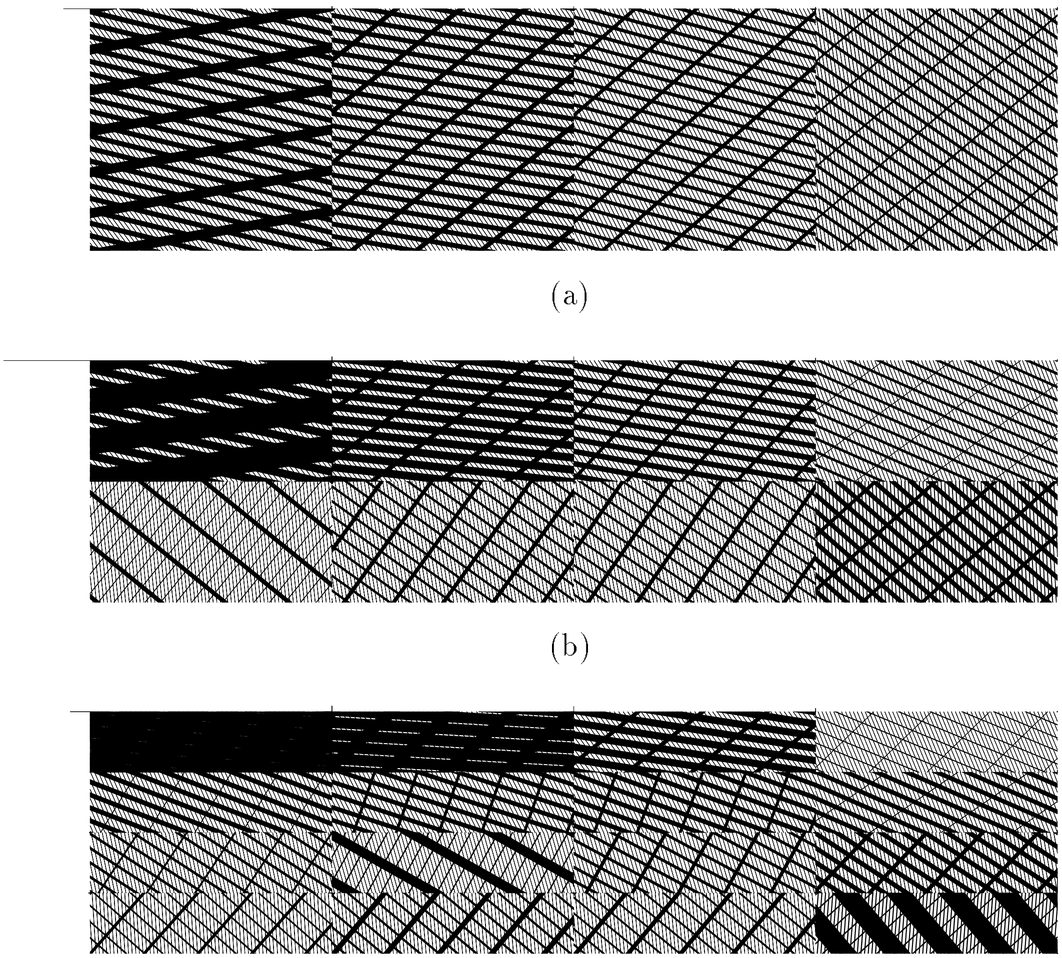

(a)

(b)

(c)

Figure 4: Optimal designs obtained using 2x4, 2x4, and 4x4 domains with constant material properties.

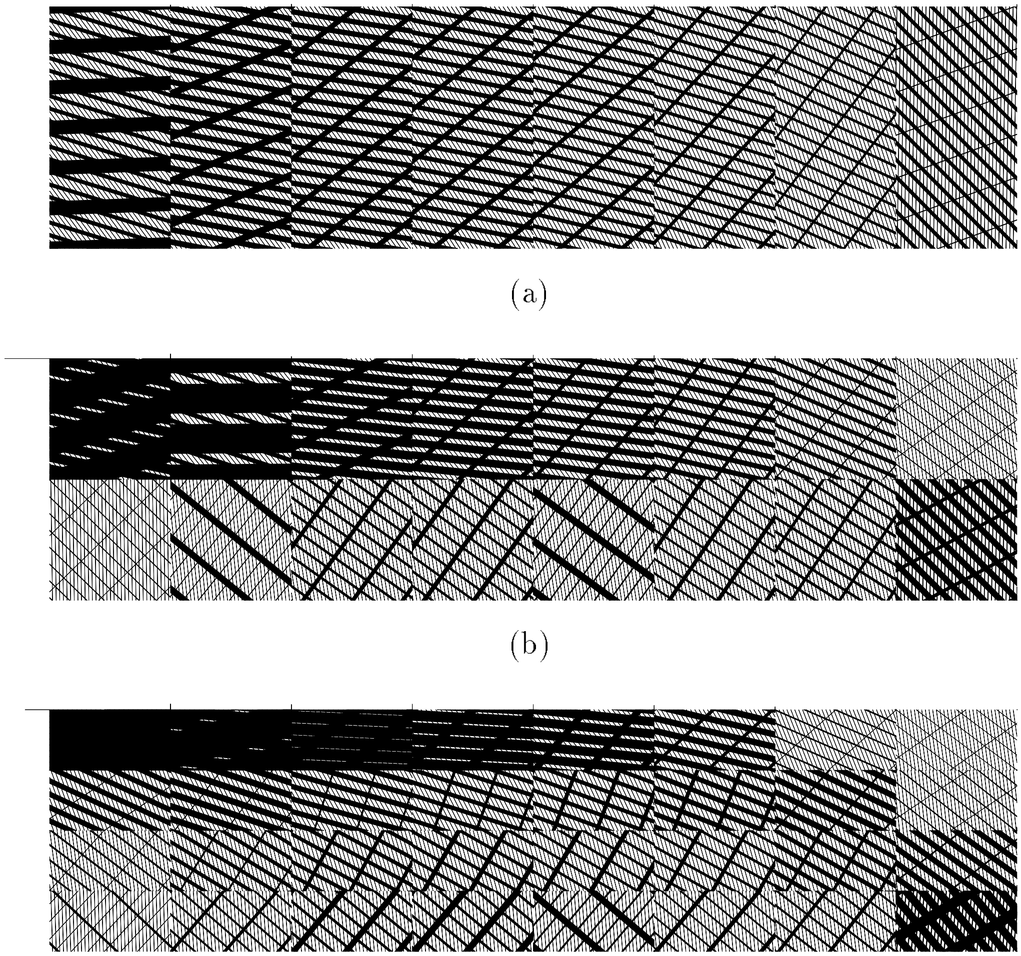

(a)

(b)

(c)

Figure 5: Optimal designs obtained using 1x8, 2x8, and 4x8 domains with constant material properties.

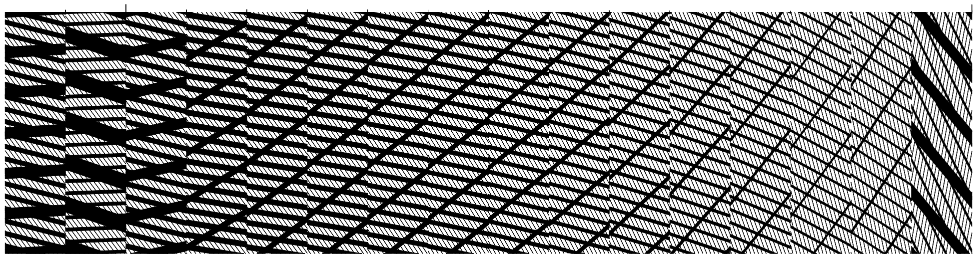

(a)

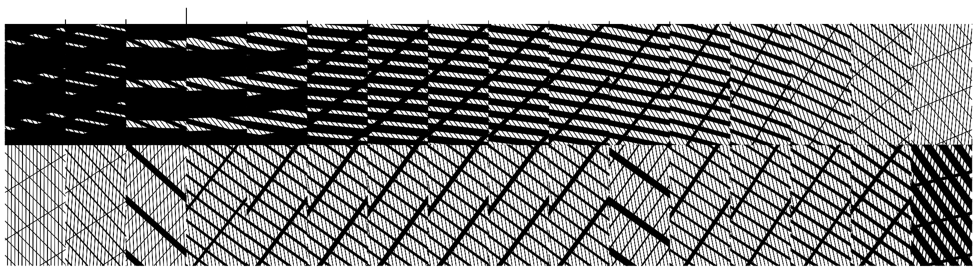

(b)

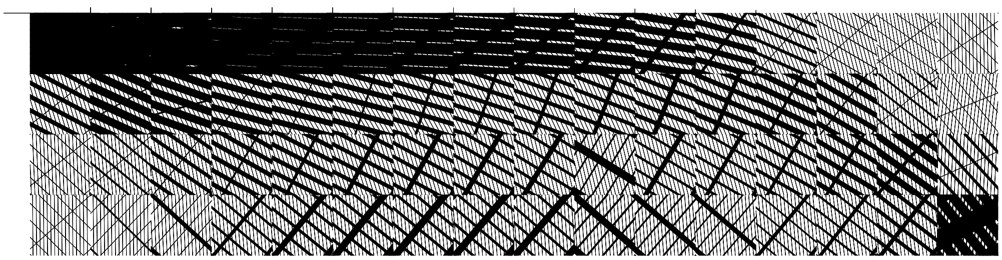

(c)

Figure 6: Optimal designs obtained using 1x16, 2x16, and 4x16 domains with constant material properties.

References

[1] Mróz, Z. Variational Methods in Sensitivity Analysis and Optimal Design. In *Second European Solid Mechanics Conference*, pages 115–147. European J. Mech. A Solids, 1994.

[2] Gibiansky, LV; Cherkaev, AV. Design of Composite Plates of Extremal Rigidity. In Cherkaev, A; Kohn, R, editors, *Topics in Mathematical Modelling of Composite Materials*, pages 95–137. , Birkhauser, 1997. Translation from Russian, Ioffe Physico-Technidal Institute, Academy of Sciences of USSR, Publication 914, 1984.

[3] Avellaneda, M. Optimal Bounds and Microgeometries for Elastic Two-Phase Composites. *SIAM J. Appl. Math.*, 47(6):1216–1228, 1987.

[4] Avellaneda, M; Milton, GW. Bounds on the Effective Elastic Tensor of Composites based on Two-Point Correlations. In Hui, D; Kozik, TJ, editors, *Composite Material Technology*, pages 89–93. ASME, 1989.

[5] Lipton, R. On Implementation of Partial Relaxation for Optimal Structural Compliance Problems. In Pedersen, P, editor, *Optimal Design with Advanced Materials*, pages 451–468, Lyngby, Denmark, 1993. IUTAM, Elsevier, Amsterdam, The Netherlands.

[6] Diaz, A; Lipton, R; Soto, CA. A New Formulation of the Problem of Optimum Reinforcement of Reissner-Mindlin Plates. *Comp. Meth. Appl. Mechs. Engrg*, 1994.

[7] Gibiansky, LV; Cherkaev, AV. Microstructures of Composites of Extremal Rigidity and Exact Bounds on the Associated Energy Density. In Cherkaev, A; Kohn, R, editors, *Topics in Mathematical Modelling of Composite Materials*, pages 273–317. , Birkhauser, 1997. Translation from Russian, Ioffe Physico-Technidal Institute, Academy of Sciences of USSR, Publication 1115, 1987.

[8] Bendsøe, MP. Optimal Shape Design as a Material Distibution Problem. *Struct. Optim.*, 1:193–202, 1989.

[9] Bendsøe, MP. *Optimization of Structural Topology, Shape, and Material.* Springer-Verlag, Heidelberg, Germany, 1995.

[10] Rozvany, GIN; Bendsøe, MP; Kirsch, U. Layout Optimization of Structures. *Applied Mechanics Reviews*, 48:41–119, 1995.

[11] Francfort, GA; Murat, F. Homogenization and Optimal Bounds in Linear Elasticity. *Arch. Rat. Mech. Anal.*, 94:307–334, 1986.

[12] Pedersen, P. On Optimal Orientation of Orthotropic Materials. *Struct. Optim.*, 1:101–106, 1989.

[13] Lipton, R; Diaz, A. Moment Formulations for Optimum Layout in 3D Elasticity. In Olhoff, N; Rozvany, GIN, editors, *Structural and Multidisciplinary Optimizatio n*, pages 161–168, Goslar, Germany, 1995. Pergamon, Oxford, UK, 1995.

[14] Krog, LA; Olhoff, N. Topology and Reinforcement Layout Optimiza tion of Disk, Plate and Shell Structur es. In Rozvany, GIN, editor, *Topology Optimization in Structural Mechan ics*, pages 237–322, Udine, Italy, 1997. CISM, Springer-Verlag, Wien, 1997.

[15] Krein, MG; Nudelman, AA. *The Markov Moment Problem and Extremal Problems.* Translation of Mathematical Monographs, 50. American Mathematical Society, 1977.